Proceeding Series of the Brazilian Society of Computational and Applied Mathematics, v. 10, n. 1, 2023.

Trabalho apresentado no XLII CNMAC, Universidade Federal de Mato Grosso do Sul - Bonito - MS, 2023

Proceeding Series of the Brazilian Society of Computational and Applied Mathematics

A brief discussion on the choice of a model to simulate drill-string dynamics

H. Goicoechea[1], R. Lima [2], R. Sampaio [3]
Pontificia Universidade Católica, Rio de Janeiro, RJ
F. Buezas[4]
IFISUR-Conicet, Bahía Blanca, Argentina

Abstract. A comparison of the dynamics obtained using two different models of a drill-string is made. A structure that is 1200 m long is analysed. In the first model, a two degrees-of-freedom (DOF) approach is used, where 1-axial DOF and 1-torsional DOF are considered. This model has been widely used in the literature. The second model maintains the 1-DOF axial formulation and employs a wave-equation for the torsional part. In both cases, the structural dynamics are coupled with the dynamics of the cutting through the depth-of-cut used in the bit-rock interaction relation. To calculate the previous depth, an advection equation is solved along with the equations of motion. One application case is simulated. The results show that the dynamics differ considerably. This suggests that the second model, with a continuous torsional shaft, could be capturing aspects of the dynamics that are neglected in the 2-DOF approach.

Palavras-chave. Drill-string dynamics, soil cutting, advection equation in cutting, torsional oscillations, stick-slip

1 Introduction

Drill-strings are very slender structures used in the extraction of oil and gas that may undergo complex dynamics, exhibiting vibrations and stick-slip, as in [3], as well as buckling and other phenomena.

In relation with their modelling, both discrete and continuous models are found in the literature. For instance, [4] presents a 2 degrees-of-freedom (DOF) model to study the cause of drill-string stick-slip vibrations. The model introduces a novelty in comparison to previous research: instead of adopting a classical velocity-dependent bit-rock formulation, it proposes a velocity-independent approach. This way, the research of [4] showed that rate-independent bit-rock formulations can better explain the origin of the stick-slip vibrations in drill-strings. The results show that self-excited stick-slip vibrations can also arise as a consequence of the regenerative cutting (that is, the successive cutting over a wavy surface), reproducing the results observed by previous researchers, although this time they are not justified through velocity-dependent rock parameters which, given that other research claims to not have found such behaviour in other experimental tests, could be unrealistic.

Examples of continuous models are found in [1, 5], to name some.

Given the different formulations found across studies concerning drill-string dynamics, there is no clear consensus towards the choice of an optimal model for drill-strings. This choice might be

[1]h.e.goicoechea@gmail.com / egoicoechea@ifisur-conicet.gob.ar
[2]robertalima@puc-rio.br
[3]rsampaio@puc-rio.br
[4]fbuezas@ifisur-conicet.gob.ar

motivated by the integration run-time, simplicity, or the capacity to tackle the problem analytically, a task that is often more difficult when continuous formulations are employed. The aim of this work is to show that a 2-DOF model to simulate the dynamics of a real scale drill-string may result in an oversimplification of the problem. This will be shown through a comparison between two different models. The analysis presented in this article is an excerpt of the work carried out in [2].

2 The drill-string models

In this study, the predictions obtained by two different models, namely M1 and M2, will be compared. A sketch showing the details of each model is provided in Fig. 1.

Model M1 is based on the formulation developed by [4], although some changes in the implementation were made, with the observation that the simulations do not present appreciable differences with regards to the original simulations.

Model M2 is similar to M1, although the torsional dynamics are tackled with a continuous formulation while retaining a 1-DOF approach for the axial motion.

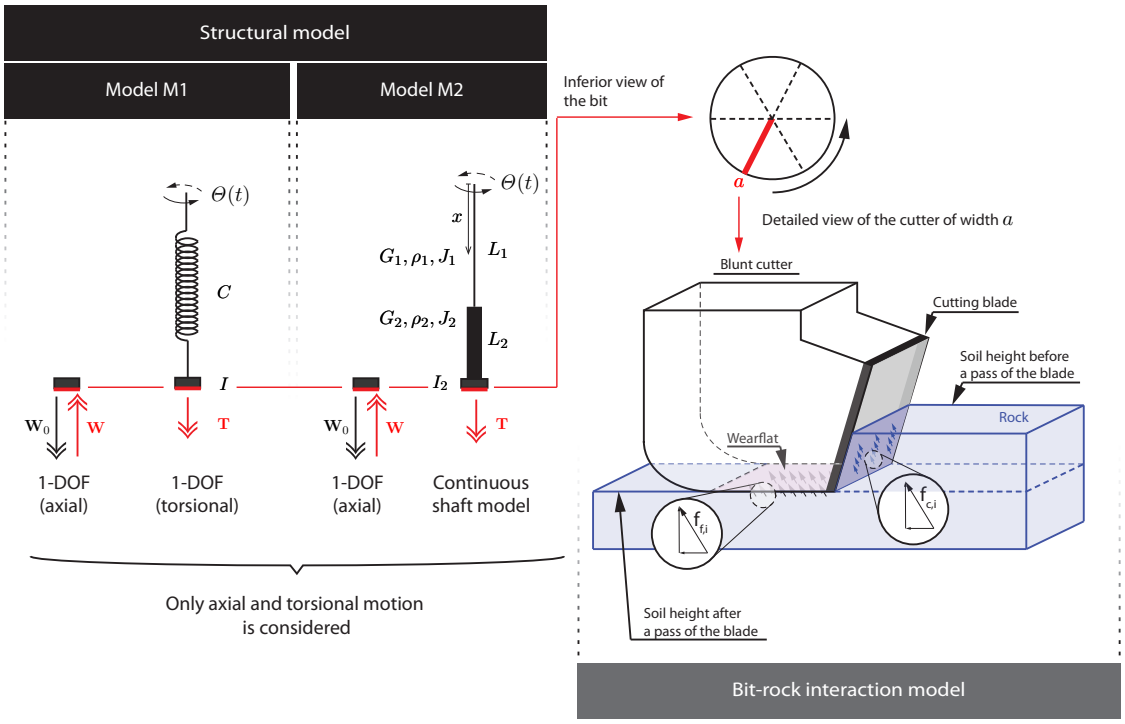

Figure 1: A sketch showing the two models employed, M1 and M2. Model M1: M is a mass, I an inertia, C a spring constant. Model M2: two different cross-sections are considered with J_1, J_2 being the geometric moment of inertia of the drill-pipes and the bottom hole assembly (BHA), respectively; G_1, G_2 the shear elastic moduli; and ρ_1, ρ_2 the densities of the material. At the lower end, a concentrated inertia I_2 is considered. $\mathbf{W}, \mathbf{W}_0$ and $\mathbf{T}$ are generalised forces.

2.1 Model M1 (2-DOF)

The axial and torsional dynamics of the model are given by (1). In that equation, U is the position of the bit, W_0 is the magnitude of the difference between the submerged weight and the hook load and W the magnitude of a reaction force due to the bit-rock interaction, Φ is the angular displacement of the bit, C a spring constant to account for the rigidity of the drill-pipes, I the concentrated inertia to account for the bottom hole assembly (BHA) and T the torque-on-bit due to the bit-rock interaction.

$$M\frac{d^2U}{dt^2} = W - W_0, \quad I\frac{d^2\Phi}{dt^2} + C(\Phi - \Theta) = T \tag{1}$$

2.2 Model M2 - (semicontinuous)

The axial and torsional dynamics of M2 are modelled by (2). Recalling that in M2 the axial dynamics retain the same formulation used in M1. For the torsional dynamics, $x_1 \in [0, L_1]$, and $x_2 \in [L_1, L_1 + L_2]$, G_j are shear moduli, J_j are geometric moments of inertia, ρ_j are the material densities.

$$M\frac{d^2U}{dt^2} = W - W_0, \quad G_jJ_j\frac{\partial^2\Phi_j}{\partial x_j^2} = \rho_jJ_j\frac{\partial^2\Phi_j}{\partial t^2}, \text{with } j = \{1, 2\}. \tag{2}$$

Also, the following boundary conditions in (3) are used, with $\Phi_j = \Phi_j(x_j, t)$ being the angular displacement of the column, $\Theta(t)$ an imposed rotation at the top, T the torque-on-bit due to the bit-rock interaction.

$$\begin{aligned}
&\Phi_1(x_1 = 0, t) = -\Theta(t), \;\; \Phi_1(x_1 = L_1, t) = \Phi_2(x_2 = L_1, t) \\
&G_1J_1\frac{\partial\Phi_1}{\partial x_1}(x_1 = L_1, t) = G_2J_2\frac{\partial\Phi_2}{\partial x_2}(x_2 = L_1, t) \\
&G_2J_2\frac{\partial\Phi_2}{\partial x_2}(x_2 = L_1 + L_2, t) = T - I_2\frac{\partial^2\Phi_2}{\partial t^2}(x_2 = L_1 + L_2, t)
\end{aligned} \tag{3}$$

3 The bit-rock interaction model

The elements considered in the bit-rock interaction model are depicted in Fig. 2, where a sketch of a blunt cutter is shown. The magnitude of the forces and torques are obtained by integration over the contact regions $A_{f,i}$ and $A_{c,i}$. The bit-rock formulation is based on four elements whose functional form is depicted in Fig. 2 : a rock contact strength function $\sigma = \sigma(\omega_b, v_b)$, defined in terms of two contact strength parameters σ_1 and σ_2, and the small regularisation constants c_1 and c_2; a rock intrinsic specific energy function (which should be better called a cutting strength function) $\epsilon = \epsilon(\omega_b)$, that depends on the intrinsic specific energy parameter ϵ_1 and a regularisation constant c_3; the cutter inclination coefficient ζ; and the coefficient of friction μ. In the previous expressions, ω_b and v_b are the torsional and axial speed of the bit.

For a symmetric and equiangular distribution of blades with radius $a_i = a$, depth of cut $d_i = d$, wearflat length $l_i = l$, for $i = \{1, \dots, n_b\}$, the total force and torque for the n_b blades is

$$\mathbf{W} = \mathbf{W}_c + \mathbf{W}_f, \;\; \mathbf{W}_c = \epsilon(\omega)\zeta a d n_b \mathbf{n}, \;\; \mathbf{W}_f = \sigma(\omega, v) a l n_b \mathbf{n} \tag{4}$$

$$\mathbf{T} = \mathbf{T}_c + \mathbf{T}_f, \;\; \mathbf{T}_c = \frac{1}{2}\frac{a}{\zeta}\mathbf{W}_c, \;\; \mathbf{T}_f = \frac{1}{2}a\mu\gamma\mathbf{W}_f \tag{5}$$

DOI: 10.5540/03.2023.010.01.0006

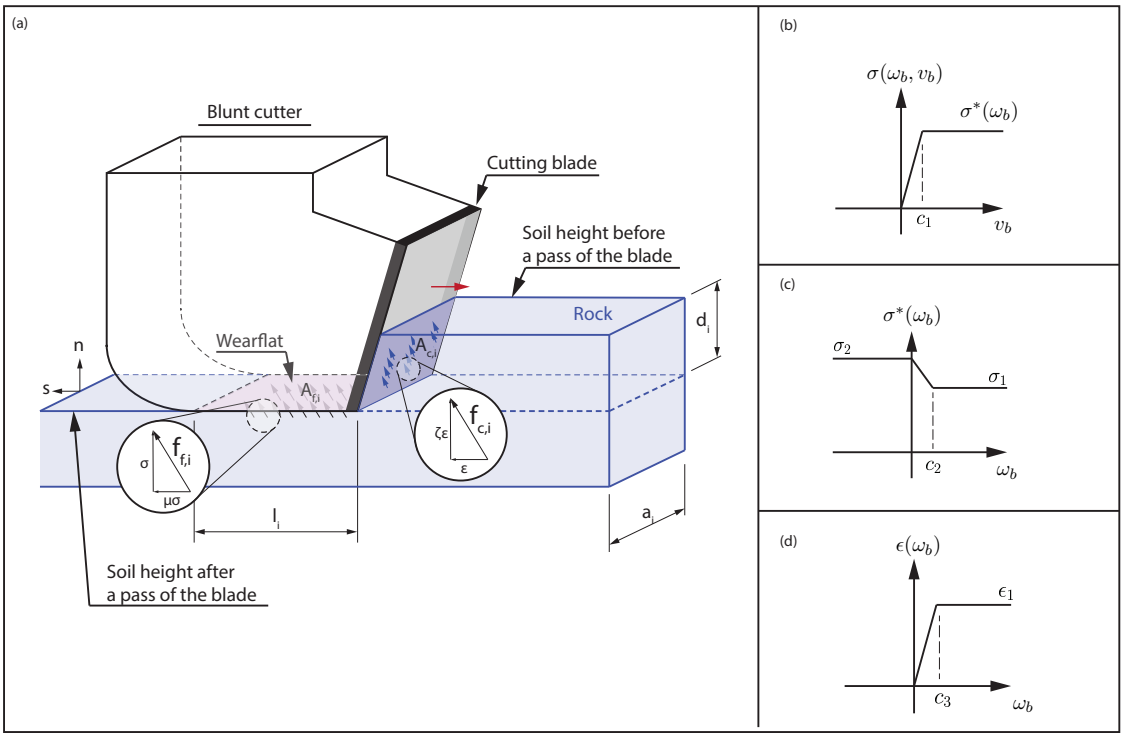

Figure 2: (a) A sketch showing the geometry of the single cutter i is shown, as well as some of the elements that are taken into account in the bit-rock interaction model; (b) to (d) functional forms adopted for the bit-rock parameters.

Finally, the previous expressions (4) and (5) require the calculation of the depth-of-cut, d. This is tackled by solving an extra PDE to account for the cutting process, an advection equation.

3.1 Solving the dynamics of the cutting process

The previous forces depend on the calculation of an instantaneous depth-of-cut. Its magnitude is obtained by solving an advection equation altogether with the previous equations of motion. If $L_s(\eta, t)$ indicates the position of the soil profile, the equation takes the form

$$\frac{\partial L_s}{\partial t} + \omega \frac{\partial L_s}{\partial \eta} = 0, \quad \text{with } \eta \in \left[0, \frac{2\pi}{n_b}\right] \tag{6}$$

where n_b is the number of blades. The boundary conditions are

$$\text{If } \omega_b(t) \geq 0, \quad L_s(\eta = 0, t) = \begin{cases} U(t), \ L_s(\eta = \dfrac{2\pi}{n_b}, t) < U(t) \\ \\ L_s(\eta = \dfrac{2\pi}{n_b}, t), \ L_s(\eta = \dfrac{2\pi}{n_b}, t) \geq U(t) \end{cases} \tag{7}$$

$$\text{or if } \omega < 0, \quad L_s(\eta = \frac{2\pi}{n_b}, t) = L_s(\eta = 0, t),$$

which means that cutting can only occur if the bit is rotating in the positive direction ($\omega_b > 0$). In the previous equations, $U(t)$ is the position of the bit. Finally, at all times the instantaneous depth of cut is given by

$$d_i = \max\Big\{L_s\Big(\eta = \frac{2\pi}{n_b}, t\Big) - L_s\Big(\eta = 0, t\Big), 0\Big\} \tag{8}$$

4 The initial conditions

The two models admit a solution that is non-oscillatory if a constant angular speed is imposed at the top such that $\Theta(t) = \Omega_0 t$. This solution is used as the initial condition in all cases, with exception of the angular speed where a small perturbation is considered. See [2] for more details.

5 Simulations: comparison between the predictions of the two models

		Real structure	Model M1	Model M2
Property	Description			
L_1	Drill-pipe length	1000 m	spring (C)	1000 m
L_2	BHA length	200 m	rigid	200 m
N_1	Number of elements (torsion)	-	–	64
N_2	Number of elements (advection)	-	64	64
I, I_2	Lumped inertia	-	$I = 112.67$ kgm^2	-
C	Rigidity parameter	-	469.05 Nm/rad	-
ρ, ρ_1, ρ_2	Density	7800 kg/m^3		
r_{po}	Drill-pipe external radius	63.5 mm		
r_{pi}	Drill-pipe internal radius	54.0 mm		
r_{co}	Collar external radius	76.2 mm		
r_{ci}	Collar internal radius	28.0 mm		
G_1, G_2	Shear modulus	77 GPa		
a	Bit radius	108.0 mm		
l	Drill-bit wearflat length	1.2 mm		
ϵ_1	Rock intrinsic specific energy	0.252 GPa		
σ_1	Rock contact strength	0.252 GPa		
ϵ_2	Rock intrinsic specific energy	0.504 GPa		
σ_2	Rock contact strength	0.504 GPa		
M	Lumped mass	24614.40 kg		
Ω_0	Imposed angular speed	14.42 rad/s		
γ	Drill-bit geometry parameter	1.00		
ζ	Cutter inclination coefficient	0.38		
μ	Coefficient of friction	0.80		
c_1	Regularisation constant	$1 \cdot 10^{-5}$		
c_2	Regularisation constant	$1 \cdot 10^{-1}$		
c_3	Regularisation constant	$1 \cdot 10^{-3}$		

Table 1: List of parameters employed in the simulation. (*) This parameter varies.

The parameters employed in this simulation are shown in Tab. 1. A graph overlaying the results for M2 and M1 is shown in Fig. 3, and a zoomed version is shown in Fig. 4. The behaviour changes substantially from one model to another: it is apparent that the frequency content is different.

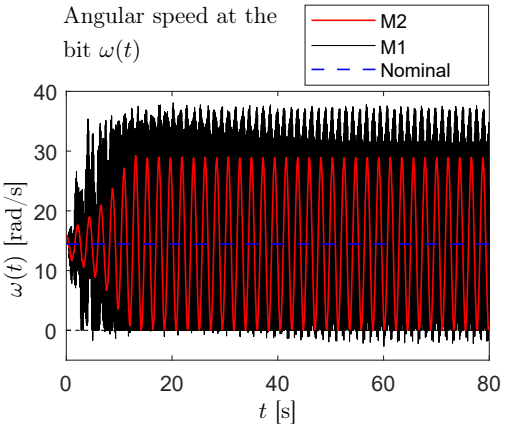

Figure 3: Simulation C1. Angular speed at the bit $\omega(t)$ for the cases C1-A and C1-B (models M1 and M2, respectively). The nominal angular bit speed is shown in dashed line.

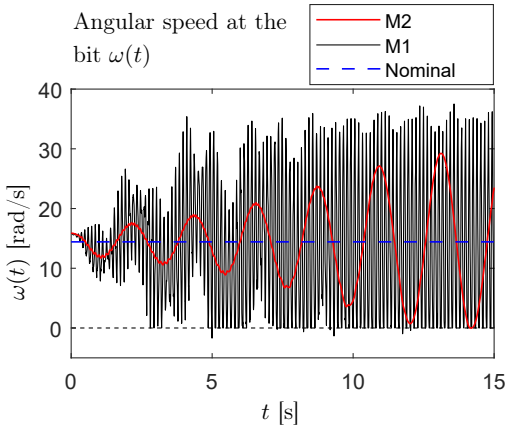

Figure 4: Simulation C1. Angular speed at the bit $\omega(t)$ for the cases C1-A and C1-B (models M1 and M2, respectively). Zoom for $t \in [0\text{s}, 10\text{s}]$. The nominal angular bit speed is shown in dashed line.

The frequency spectrum of the signal associated to the angular speed is depicted in Figs. 5 and Fig. 6, for $t > 50s$, after the transient effects vanish. The results from model M1 contain a main frequency that matches the fundamental one (0.45Hz). This is different for model M2, where the main frequency is close to the sixth natural frequency (7.40Hz), and the amplitudes associated to frequencies close to 0.45Hz are negligible, which explains the appreciable difference observed with the signals in the time-domain.

With regards to the run-time of the simulations, the calculations with M1 took 1 h 49 min, while for M2 3 h 56 min, showing an increase of 45%, recalling that 64 elements have been used for the torsional wave equation.

6 Final considerations

Given the variety of models found in the literature, the choice of an appropriate formulation is not obvious, especially when long columns are simulated. One of the motivations of this work is to discuss the benefits and drawbacks of using either a low-dimensional lumped model or a continuous one. To do this, the predictions of an established 2-DOF approach were compared with those of another model that considers a continuous torsional formulation plus 1-DOF for the axial dynamics. These models were named M1 and M2, respectively.

The results for the scenario that was simulated were dissimilar, as the responses did not match either in the time domain or the frequency domain.

The semi-continuous model M2 predicted an angular speed where, in comparison with the results with M1, higher frequencies are present. Although it has not been included due to the constraints on the length of this article, it can be shown that model M1 is contained in model M2 (if quasi-static assumptions are adopted, the formulation can be reduced to that of M1). In that context, the differences show that the discrete model M1, and that of [4], are not accurate representations of the continuous one. For this reason, the higher frequencies found with M2 provide a hint in the direction of assuring that the 2-DOF could be an oversimplification of the problem, and that the approach may be inadequate to capture the dynamics of a real-scale drill-string.

DOI: 10.5540/03.2023.010.01.0006

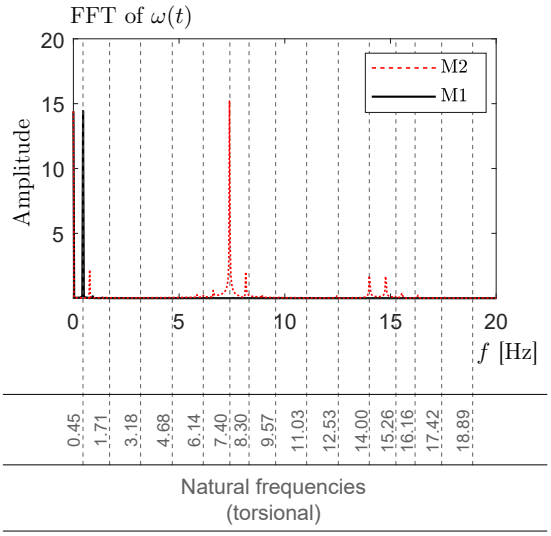

Figure 5: Simulation V2. FFT of the angular speed at the bit $\omega(t)$. Frequency range: 0 to 20Hz.

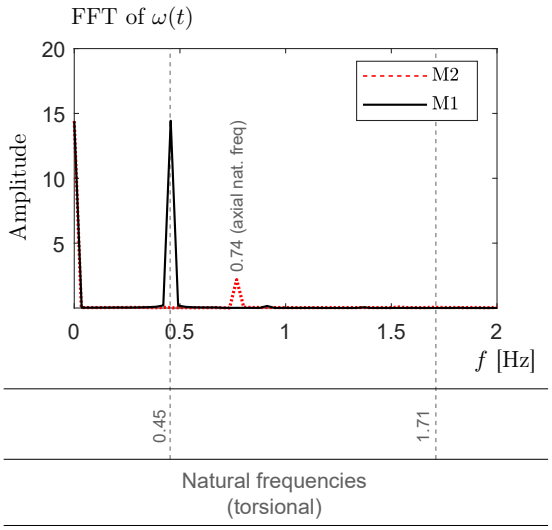

Figure 6: Simulation V2. Zoom of the FFT of the angular speed at the bit $\omega(t)$. Frequency range 0 to 2Hz.

Finally, the torsional formulation that has been used is conservative, with the exception of the forces and torques acting at the bit. Although it is not presented here, other analyses including other sources of dissipation, like internal damping, have been run. The results also indicate discrepancies in the predictions that justify the use of continuous approaches.

References

[1] H. E. Goicoechea, F. S. Buezas, and M. B. Rosales. "A non-linear Cosserat rod model for drill-string dynamics in arbitrary borehole geometries with contact and friction". In: **International Journal of Mechanical Sciences** 157-158.March (2019). Publisher: Elsevier Ltd, pp. 98–110. ISSN: 00207403. DOI: 10.1016/j.ijmecsci.2019.04.023.

[2] H. E. Goicoechea et al. "Drill-string with cutting dynamics: a mathematical assessment of two models". In: **Journal of Sound and Vibration** (Feb. 2023). DOI: 10.1016/j.jsv.2022.117364.

[3] Roberta Lima and Rubens Sampaio. "Stick-mode duration of a dry-friction oscillator with an uncertain model". In: **Journal of Sound and Vibration** 353 (2015). Publisher: Elsevier, pp. 259–271. ISSN: 10958568. DOI: 10.1016/j.jsv.2015.05.015.

[4] T. Richard, C. Germay, and E. Detournay. "A simplified model to explore the root cause of stick-slip vibrations in drilling systems with drag bits". In: **Journal of Sound and Vibration** 305.3 (2007). ISBN: 0022460X, pp. 432–456. ISSN: 10958568. DOI: 10.1016/j.jsv.2007.04.015.

[5] R. Sampaio, M. T. Piovan, and G. Venero L. "Coupled axial/torsional vibrations of drill-strings by means of non-linear model". In: **Mechanics Research Communications** 34.5-6 (2007). ISBN: 978-1-4020-4994-1, pp. 497–502. ISSN: 00936413. DOI: 10.1016/j.mechrescom.2007.03.005.

